A Hierarchical Multivariate Copula-based Framework for Cognitive Modeling

Abstract

Computational cognitive models provide a principled approach to understanding behavior and cognition by formalizing latent parameters underlying decision-making and learning. Many existing models take a univariate approach, analyzing single measures in isolation, while others incorporate multiple measures but impose specific process assumptions that constrain how these measures relate. For example, drift diffusion models (DDMs) jointly model choices and response times under the assumption that decisions arise from an evidence accumulation process. While effective in many contexts, this assumption constrains the flexibility of DDMs, potentially limiting their applicability to cognitive processes that do not conform to an accumulation-to-bound mechanism.

Here, we introduce a hierarchical multivariate modeling framework that uses copulas to flexibly combine independent likelihood functions, enabling joint modeling of multiple measures without imposing restrictive assumptions. Through simulations and empirical applications, we assess the reliability, discriminability, and advantages of copula-based modeling (CBM). Model validation via simulation-based calibration, model recovery, and sensitivity analyses demonstrate that CBM is computationally robust and accurately recovers latent parameters. When applied to psychophysical and probabilistic learning tasks, CBM can be empirically distinguished from DDMs, even with limited data. Additionally, incorporating response times improves predictive accuracy for binary choices while reducing uncertainty in parameter estimates.

This framework offers several advantages. It accommodates diverse data types, including behavioral responses, physiological signals, and neural activity, without requiring them to share the same distributional properties. It explicitly models dependencies between measures, capturing interactions typically overlooked in univariate approaches. It is theoretically agnostic, allowing for greater flexibility in modeling cognitive processes. Further, it enables more efficient use of available data by integrating multiple sources of information, while enhancing model accuracy and efficiency of parameter estimation. These findings establish CBM as a flexible and generalizable framework, broadening the scope of multivariate cognitive modeling and expanding the methodological toolkit available for cognitive science.

Keywords: Copula; Multivariate; Hierarchical; Framework

Introduction

From simple reflexes to abstract reasoning, cognition spans a wide spectrum of interacting processes, many of which remain only partially understood. The challenge of unraveling these processes lies not only in their quantification but also in developing models that accommodate the richness of cognitive phenomena while maintaining interpretability and theoretical rigor. Traditional approaches to computational modeling often rely on univariate analyses that isolate individual measures, such as choices or response times, and treat them as independent indicators of underlying cognitive mechanisms. While effective in some contexts, this approach risks discarding meaningful dependencies between variables and overlooks the interactions that shape behavior and cognition.

Computational cognitive models offer a principled framework for inference about cognitive processes by formalizing latent parameters that govern decision-making and learning. These models provide a principled approach to linking observed behavior to hypothesized cognitive mechanisms. A particularly influential class of such models, Drift Diffusion Modeling (DDM), posits that decision-making arises from an evidence accumulation process, in which noisy information accrues over time until a decision threshold is reached (Ratcliff, 1978; Ratcliff & Rouder, 1998). The DDM's ability to jointly model binary choices and response times has made it a cornerstone of cognitive modeling. However, its reliance on an accumulation-to-bound mechanism imposes a specific process assumption that may not be suitable for all cognitive tasks. For instance, continuous measurements of physiological signals such as pupil responses and brain responses.

To expand the methodological toolkit for cognitive science, we introduce Copula-Based Modelling (CBM), a hierarchical multivariate modeling framework that uses copulas to flexibly model dependencies between multiple measures. Unlike conventional approaches that impose fixed generative processes, copulas allow the integration of distinct likelihood functions while preserving the unique distributional properties of each variable (Kolev et al., 2006). By decoupling marginal distributions from dependency structures, CBM enables joint modeling of multiple measures without restrictive assumptions about their relationships. This flexibility makes CBM applicable to a broad range of cognitive science questions, allowing researchers to jointly model choices, response times, confidence ratings, physiological signals, and neural activity within a unified statistical framework.

Methods

We evaluated the copula-based modeling (CBM) framework through simulations and applications to experimental data, assessing its capacity to jointly model binary choices and response times across two decision-making paradigms. These paradigms consisted of a psychophysical task, where participants reported the presence or absence of a stimulus, and a probabilistic learning task, where participants learned cue-outcome associations. These paradigms were selected due to their prominence in cognitive science and their compatibility with the drift diffusion model (DDM) (Palmer et al., 2005; Pedersen et al., 2017). Using hierarchical Bayesian inference, we validated model specification and inference algorithms through simulation-based calibration and examined whether incorporating response times improved model fit. The framework was then applied to publicly available datasets to assess its performance on real behavioral data, with model comparisons conducted using predictive accuracy measures. These analyses allowed us to determine whether CBM improves behavioral modeling by capturing dependencies between choices and response times more effectively than DDM.

Copula-Based Modeling.

The CBM framework is built on three fundamental components. First, the relationships between experimental variables and outcome measures are represented through coupled equations with latent parameters. Second, we assign appropriate likelihood functions to each outcome measure. Third, the dependency structure among outcome measures, beyond their marginal likelihoods, is modelled using copulas.

Step 1: Modeling choice and response times in decision-making tasks.

Choice modeling in psychophysical tasks.

In the psychophysical task, participants report the presence or absence of a sensation in response to stimulus presentation. The independent variable, Xt, represents stimulus strength, and the probability of detecting a percept is modeled using a psychometric function (Klein, 2001):

$$E_t = \lambda + (1 - 2 \cdot \lambda) \cdot \frac{1}{1 + exp\left(-\beta \cdot \left(X_t - \alpha_p\right)\right)}$$

where $\mathrm{E_t}$ represents the latent expectation at trial t, reflecting the probability of reporting the presence of a percept, α_p the threshold, β the slope, and λ the lapse rate.

Choice modeling in learning tasks.

In the probabilistic learning task, participants learn associations between cues and outcomes. The independent variable, R_t, represents cue-stimulus associations, with $R_t = 1$ denoting a positive association and $R_t = 0$ a negative one. Learning follows the Rescorla-Wagner model (Rescorla & Wagner, 1972):

$$E_{t+1} = E_t + \alpha_l * (R_t - E_t)$$

where E_t represents the latent expectation at trial t, corresponding to the probability of expecting a reward, and α_l the learning rate.

Response times modelling.

Beyond binary choices, response times provide additional information into cognitive processing. Early work in chronometric functions (Hick, 1952, Hyman, 1953) demonstrated a linear relationship between response time and decision uncertainty, quantified as entropy. For binary decisions, response entropy is defined as:

$$H(E_t) = E_t \cdot log(E_t) + (1 - E_t) \cdot log(1 - E_t)$$

where $H(E_t)$ is the degree of uncertainty in an expectation at each trial. Response times are then modeled as an affine function of this entropy:

$$\widehat{RT_t} = RT_{int} + RT_{slope} \cdot H(E_t)$$

where $\widehat{RT_t}$ denotes the expected response time at trial t, RT_{int} reflects the response speed under conditions of minimal or no uncertainty, while RT_{slope} quantifies the efficiency with which subjects resolve uncertainty during decision-making, measured in seconds per bit. We further decomposed these response times into decision and non-decision components by including a non-decision time parameter in our likelihood function. This approach allows response times to be integrated into CBM as an additional dependent measure.

Step 2: Selection of likelihood functions for choice and response times data

To connect our model predictions with observed data, we use statistical likelihood functions that are appropriate for each behavioral measure.

Binary choices (B) are modelled using a Bernoulli likelihood, which is the maximum entropy distribution for binary outcomes with a known expectation.

Response times (RT) are modeled using a shifted lognormal likelihood, which ensures non-negative values and includes an additional non-decision parameter which aligns with empirical response time distributions.

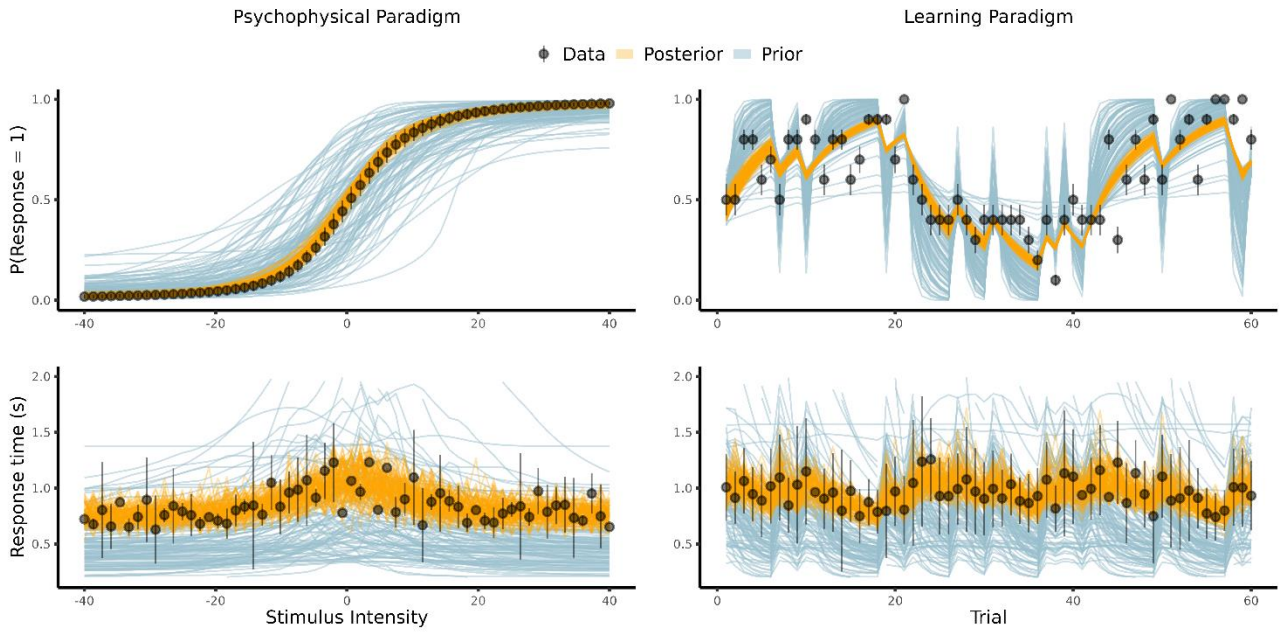

Figure 1. Simulated realizations of the psychometric model (left) and learning model (right) within the proposed multivariate hierarchical copula-based framework. Light blue lines represent 100 prior predictive distributions, while orange lines illustrate 100 posterior predictive draws. Group mean data points are displayed with 95% confidence intervals.

Step 3: Modelling interdependence with copulas

Until now, we have assumed that binary choices (B_t) and response times (RT_t) are conditionally independent given the experimentally manipulated variables $X_t \vee R_t$, such that:

$$p(B_t, RT_t \mid X_t) = p(B_t \mid X_t) \cdot P(RT_t \mid X_t)$$

However, this assumption may not always hold, as response times and choices often exhibit dependencies beyond their shared influence from X_t. To explicitly model this interdependence, we introduce copulas, which allow us to capture the joint structure of these variables while maintaining the flexibility of separate marginal distributions.

To this aim, we first apply the probability integral transform, which maps the observed outcome measures into standard uniform distributions:

$$(U_{t_1}, U_{t_2}) = (F_1(B_t), F_2(RT_t)$$

where F_1 and F_2 are the cumulative distribution functions of B_t and RT_t, respectively. Then, we apply the Gaussian copula to map dependencies between the transformed variables. This is achieved by applying the normal quantile function (inverse CDF of the standard normal distribution) to transform the uniform variables into a multivariate normal (MVN) distribution:

$$\begin{bmatrix} \Phi^{-1}(U_{t_1}) \\ \Phi^{-1}(U_{t_2}) \end{bmatrix} \sim MVN\left(\begin{bmatrix} 0 \\ 0 \end{bmatrix}, \begin{bmatrix} 1 & \rho \\ \rho & 1 \end{bmatrix}\right)$$

where $\Phi^{-1}(.)$ is the normal quantile function, and ρ represents the correlation between binary choices and response times, beyond what is explained by X_t.

This approach allows us to separate modeling of individual response distributions (marginals) from the dependency structure (copula). This flexibility is crucial when dealing with mixed data types, such as discrete (binary choices) and continuous (response times) variables. By introducing a copula, we preserve the interpretability of individual behavioral measures while capturing the latent dependencies that conventional models might overlook.

We used a Gaussian copula, whose correlation parameter ρ captures linear dependence in the transformed marginal space. This parameter quantifies residual associations between response times and choices beyond their marginal models, with positive values indicating that longer RTs are associated with higher likelihood of choosing "1." Additionally, the copula's negative entropy provides a principled lower bound on mutual information, serving as a diagnostic for dependencies not captured by simpler models or the specified marginals.

Drift Diffusion Modelling

For comparison with CBM, we also define drift diffusion models (DDMs) for each experimental paradigm. DDMs were parameterized to allow drift rate to vary, and their specification was defined as follows:

$$v_t = (E_t - (1 - E_t)) * v$$

where v_t represents the drift rate at time t, E_t latent expectation at trial t and v is a subject level scaling parameter. The joint likelihood function, incorporating both binary choice and response time, was modelled using the four parameter first passage time distribution:

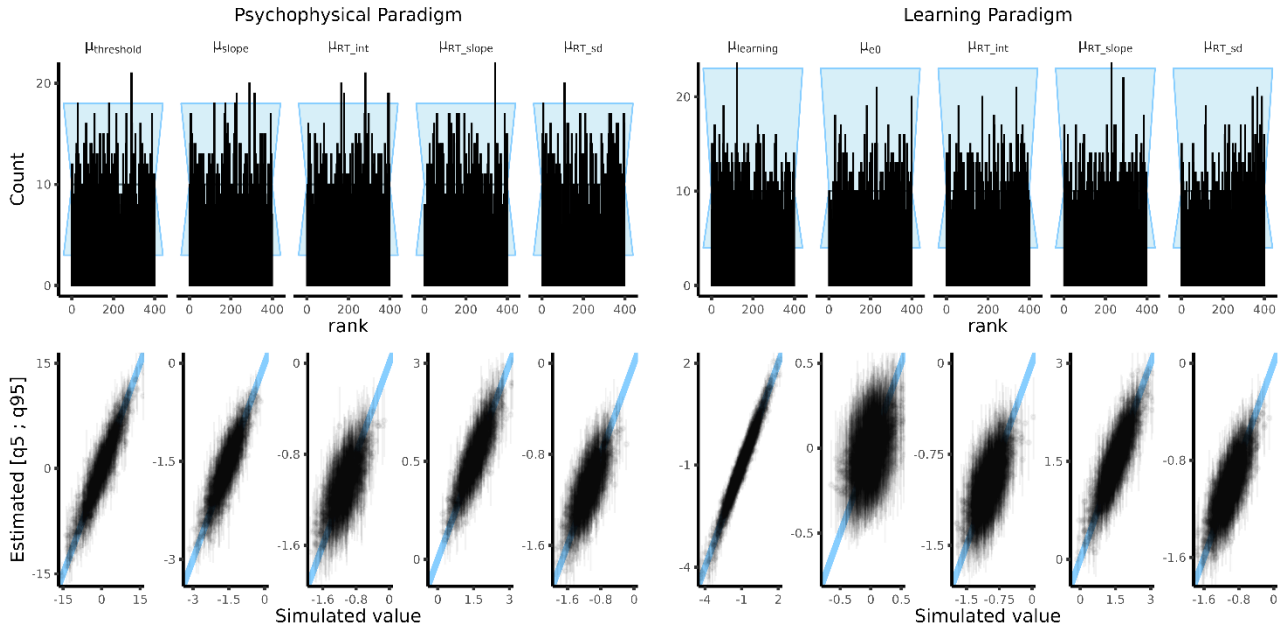

Figure 2. *Simulation-based calibration (SBC) (top) and parameter recovery (bottom) for group mean parameters in the psychometric (right) and learning (left) paradigms. SBC results display uniform histograms, indicating a well-calibrated model. The black horizontal line representing the average count and the shaded region denotes the expected 95% spread. Parameter recovery analysis compares simulated and estimated parameter values, with 90% credibility intervals shown as error bars.*

$$RT_t \sim \begin{cases} Wiener(\kappa, \delta, \eta, v_t), & B = 1 \\ Wiener(\kappa, \delta, 1-\eta, -v_t), & B = 0 \end{cases}$$

where κ is the decision boundary, δ represents non-decision time, η is the starting point bias, and v_t denotes the drift rate at time t.

Simulations

To evaluate the performance of CBM, we simulated data for both the psychophysical and learning paradigms. For the psychophysical paradigm, stimulus values were uniformly distributed between -40 and 40. For the probabilistic learning paradigm, cue-outcome associations followed reward probabilities of either 20% or 80%, with a reversal every 20 trials (Fig. 1). Each dataset included 10 subjects completing 60 trials. Subject-level parameters were drawn from group-level distributions, which were selected to align with realistic behavioral data and served as priors for model fitting. Only the non-decision time and copula correlation parameters were not drawn from hierarchical group-level distributions (see limitations). Figure 1 presents an example of the simulated dataset, illustrating samples from both the prior and posterior distributions of the CBM. A comprehensive list of prior distributions is provided in Supplementary Note and on the associated GitHub repository.

Sampling and fitting

We implemented our framework using hierarchical Bayesian inference leveraging Stan's for Hamiltonian Markov chain Monte Carlo No U-turn sampler, chosen for its flexibility in model specification, diagnostic capabilities, and incorporation of prior information. Simulations were performed in R (R Core Team 2024), and model fitting in Stan (Carpenter et al., 2017). Each model was sampled using 1000 warm-up iterations, followed by 2000 sampling iterations, with a target acceptance ratio of .95 and a maximum tree depth of 12. To ensure convergence and quality of sampled parameters, models with divergent transitions or that reached the maximum tree depth were excluded.

Simulation-based calibration

To ensure the reliability and robustness of our CBMs, we conducted simulation-based calibration (SBC) (Modrák et al., 2023, Talts et al., 2020), a method that extends standard parameter recovery (Wilson & Collins, 2019), by simulating data from the prior distribution and verifying that the estimated parameters align with the simulated values while ensuring that credibility intervals are properly calibrated. SBC provides a principled test of both the model specification and the sampling algorithm, mitigating risks associated with parameter misestimation. To implement SBC, we generated 2000 simulated datasets from the CBM for each paradigm, fitted each dataset to its corresponding model, and recorded the rank of each simulated parameter within

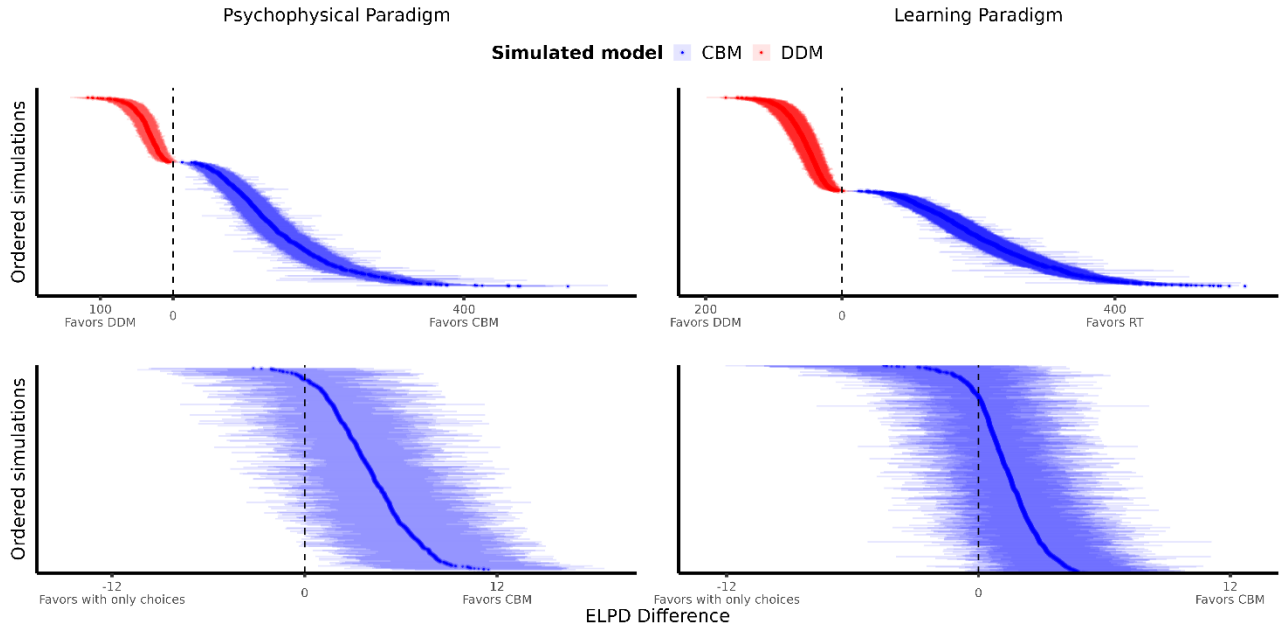

Figure 3. *Model recovery of the copula-based models (CBM) and the drift diffusion models (DDM) for psychometric (top left) and learning (top right) paradigm. Each point is a simulated dataset fitted with both models and compared on ELPD (Expected Log Predictive Density) difference indicating the discrepancy between the two models with its error (2 standard errors). Lower row depicts discrepancy between the CBM and the more traditional approach of only investigating binary choices.*

the posterior draws. We examined group mean parameters, with uniform ranks across simulations serving as confirmation that posterior credibility intervals were well-calibrated (Talts et al., 2020), meaning that an X% posterior credible interval contained the true simulated value in X% of cases (Fig. 2)
To reduce the effects of autocorrelation, which could distort rank histograms, we thinned Markov chains by a factor of 20 (Talts et al., 2020). In addition, we conducted parameter recovery by generating scatter plots comparing simulated and estimated parameter values, including 90% credible intervals, with alignment along the identity line (y = x) serving as an indicator of accurate parameter estimation.

Simulation-based analysis

Beyond SBC, we conducted an additional simulation-based analysis to systematically evaluate the comparative performance of CBM and DDM. Further, we also examined whether incorporating response times in CBM improves model fit and parameter estimation relative to models relying solely on binary choice data. To this end, we generated 1000 additional datasets for each paradigm, with the generative model set as either CBM or DDM.

We tested the discriminability of CBM against the DDM on the full trial-wise log likelihood using approximate leave-one-out cross-validation (LOO-CV) (Vehtari et al., 2017). Further to understand the influence of improvements in model fit on the binary choices, we compared the predictive accuracy of models with and without response times also using LOO-CV. Lastly, we examined the impact of response times on the posterior dispersion of key parameters, including the threshold, slope, and lapse rate for the psychometric function and the learning rate and initial expectation for the psychometric paradigm.

Applications to experimental data

To evaluate the performance of our CBM-derived models against the DDM using real experimental data, we analyzed two publicly available datasets from psychophysical and probabilistic learning paradigms.

The psychophysical dataset was sourced from the “confidence database” (Rahnev et al., 2020), specifically from Bang et al. (2019). This dataset included 12 participants performing an orientation detection task, where they were required to indicate whether a Gabor patch was present in the first or second stimulus interval. The stimulus intensity was systematically manipulated by replacing a proportion of the Gabor patch pixels with noise pixels, a method commonly used in perceptual learning studies. For the present analysis, we focused exclusively on the first day of Experiment 1.

The probabilistic learning dataset was obtained from Hess et al. (2024), in which 59 subjects completed a speed-incentivized associative reward learning task. In this experiment, participants learned to associate fractals with momentary rewards, reflecting a structured probabilistic learning environment.

For both datasets, we adjusted the prior distributions for the CBM and DDM-derived models to ensure that they were appropriately aligned with the

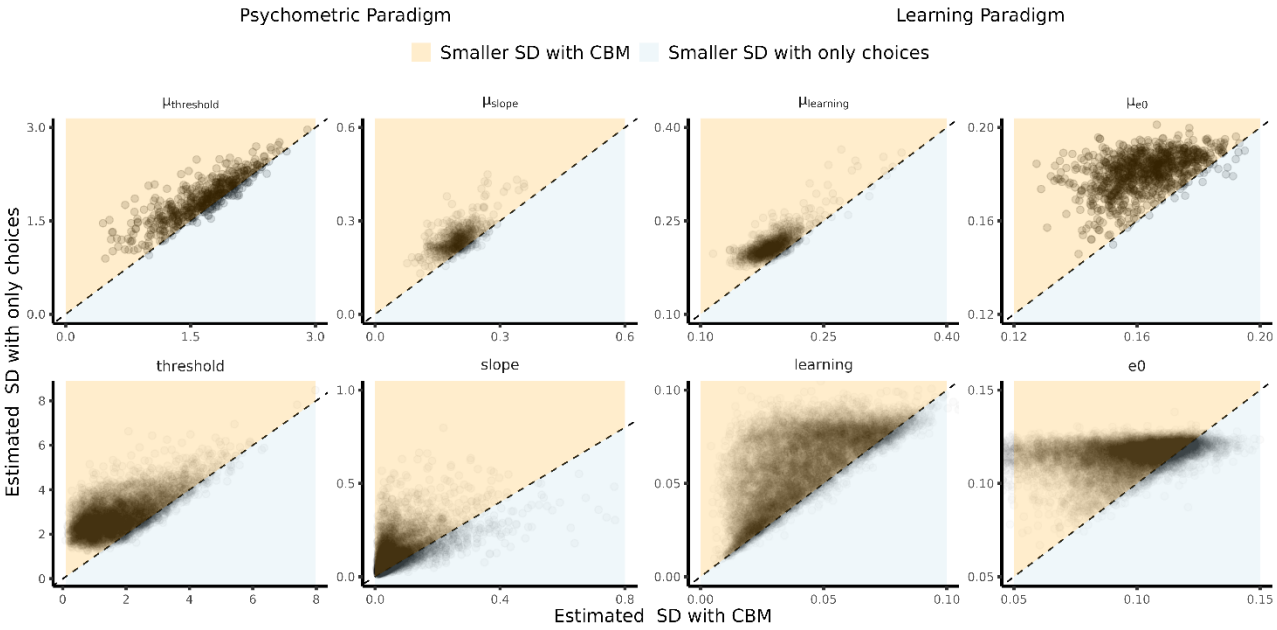

Figure 4. *Posterior standard deviation (SD) of group-level (top row) and subject-level (bottom row) parameters as a function of response time inclusion. Parameters from the psychometric paradigm (first two columns) and the learning paradigm (last two columns) are displayed. Each point in the top row represents a single dataset simulation, while each point in the bottom row corresponds to one of ten simulations per dataset. Points in the beige region indicate reduced SD when response times were included, whereas points in the light blue region indicate lower SD when response times were excluded.*

task structure and expected parameter ranges. A comprehensive list of priors is provided in

Supplementary Note. Additionally, for diagnostic reasons, we excluded the fastest response time for each participant, as these trials introduced potential issues in model comparison procedures.

Results

Computation time and dataset exclusion

Table 1 presents the median and interquartile range of computation times in seconds for each model. Due to divergent transitions or the maximum tree depth reached during sampling, 26% of datasets were excluded for the psychophysics paradigm and 2.3% for the learning paradigm.

Table 1. Computation time (median ± interquartile range)

Paradigm	Choice (s)	DDM (s)	CBM (s)
Psychophysics	6 ± 1.9	150 ± 19	351 ± 189
Learning	3.2 ± 1	110 ± 22	323 ± 154

Simulation-based calibration

Figure 2 presents the results of simulation-based calibration (SBC) and parameter recovery for the psychometric and learning paradigms. SBC results are shown as histograms, indicating where the simulated parameter values fall within the posterior draws. SBC is considered successful when these ranks are uniformly distributed, meaning that histogram heights remain within the expected 95% deviation range (shaded region). In addition to visual inspections of the histograms, we calculated the χ^2-statistic for the difference between observed and expected frequencies for each group mean parameter. This allowed us to test whether there was a significant violation of uniformity for each parameter. All p-values associated with the χ^2-statistic were above .05. Below the SBC results, parameter recovery plots assess whether estimated parameters align with simulated values. Accurate recovery is indicated by data points aligning with the identity line (y = x), confirming that the model can recover true parameter values. These results establish the validity of the model implementation.

Model recovery analysis

Model recovery analysis assessed the ability to distinguish between CBM and DDM (Fig. 3 upper). In the psychophysical paradigm, the generative model was correctly identified in nearly all cases. For DDM-generated data, the model was correctly selected 95% of the time. For CBM-generated data, model recovery was nearly perfect at 99.8%.

Model recovery was just as definitive in the learning paradigm. For DDM-generated data, the model was correctly identified in 99% of cases. For CBM-generated data, the model selection rate was 100%.

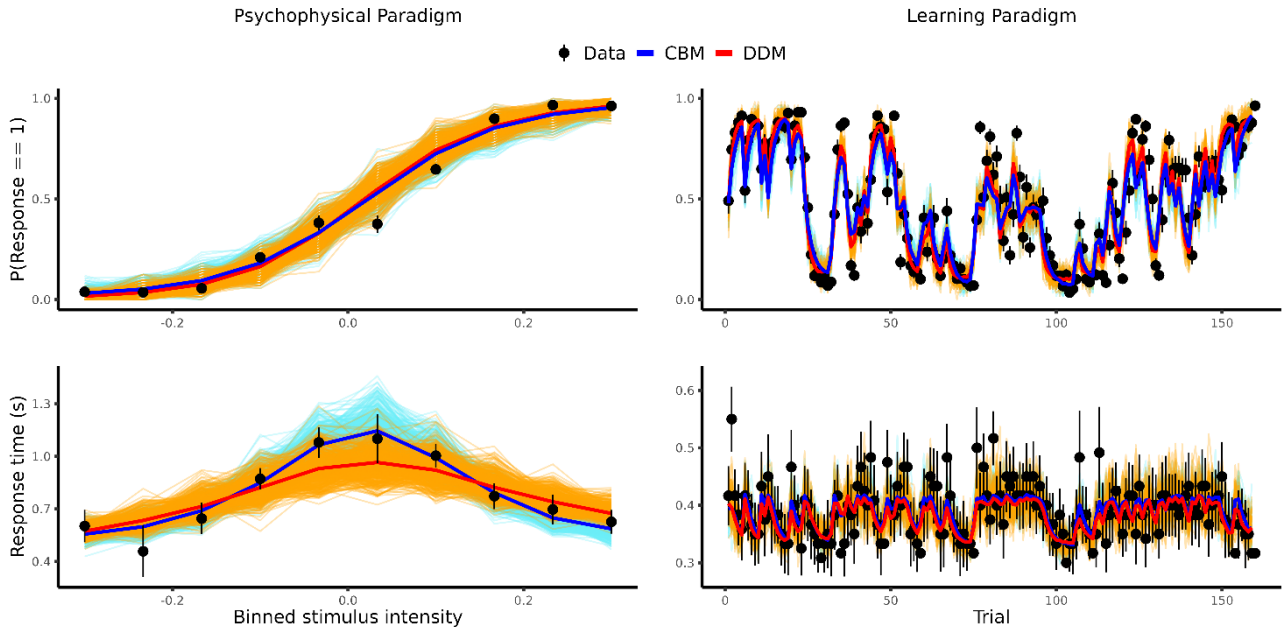

Figure 5. *Posterior predictive checks for experimental data from a psychometric paradigm (left) and a learning paradigm (right). Group-averaged data are shown as black dots with 95% confidence interval. The top row depicts the probability of a response, while the bottom row presents response times. Marginal posterior means and medians are shown for both the drift diffusion model (DDM) (red) and the multivariate hierarchical copula-based framework (CBM) (blue). Orange and light blue lines represent 500 marginal posterior draws for DDM and CBM, respectively, illustrating uncertainty around the conditional mean and medians (thick lines).*

Table 2. Percentage of correct model identifications[1]

Paradigm	DDM	CBM
Psychophysics	95 [92;96] %	99.8 [99;100] %
Learning	99 [98;99] %	100 [99;100] %

Modelling choices and response times

The lower part of figure 3 compares model fits for CBM with and without response times. Models that incorporated response times were generally favored (Table 3).

Table 3. Percentage for models on binary choices

Paradigm	Choice only	CBM
Psychophysics	0 [0;0.01] %	37 [33;41] %
Learning	0 [0;0.01] %	13 [11;16] %

To assess how response times influenced posterior parameter estimates, Figure 4 presents pairwise scatter plots for group-level and subject-level estimates. Across most simulations, posterior dispersion was reduced when response times were included, as indicated by lower standard deviations. This suggests that incorporating response times improves the precision of parameter estimates.

Experimental data

Posterior predictive checks for both paradigms and models are presented in Figure 5. Model comparison analysis indicated that CBM-derived models were significantly favored over the DDM, with an expected log pointwise predictive difference (elpd difference ± se difference) of -153 ± 17 for the psychophysical paradigm and -554 ± 48 for the learning paradigm.

When considering predictive performance based solely on binary choices, the comparisons did not reveal significant preferences, yielding values of -1.5 ± 1.7 for the psychophysical paradigm and -11 ± 6 for the learning paradigm. The psychophysical paradigm exhibited a preference for CBM, while the learning paradigm showed a preference for the model without response times.

Additional details, including trace plots, prior-posterior updates, subject level posterior predictive fits model comparison diagnostics and correlation matrix between the two models, are provided in Supplementary Figures 1-10 and Supplementary Table 1.

[1] Uncertainty was computed by updating a beta distribution starting from Beta (1,1).

Discussion

The findings from this study demonstrate that the copula-based modeling (CBM) framework provides a flexible and robust approach to multivariate cognitive modeling by accommodating dependencies between measures without imposing restrictive assumptions. Through simulations and applications to empirical data, CBM showed strong reliability, parameter recovery, and discriminability, establishing it as a valuable alternative to traditional models such as the drift diffusion model (DDM).

A key advantage of CBM is its ability to integrate heterogeneous data sources while maintaining theoretical flexibility. In contrast to DDM, which relies on an evidence accumulation framework to jointly model choices and response times, CBM allows for the independent specification of marginal distributions while capturing interdependencies via copulas. This distinction enables CBM to model decision-making processes that do not necessarily adhere to an accumulation-to-bound mechanism. The simulation-based calibration and model recovery analyses confirmed that CBM accurately estimates latent parameters and can be distinguished from DDM.

Beyond model discriminability, the inclusion of response times in CBM improved predictive accuracy for binary choices while reducing uncertainty in parameter estimates. This was evidenced by the reduced posterior dispersion of key parameters when response times were incorporated. This suggests that response times contribute meaningful information about underlying cognitive processes and should be included in modeling frameworks where feasible. These findings align with prior work demonstrating that response times serve as valuable indicators of uncertainty and decision-making strategies, complementing choice data (Hess et al., 2024).

Moreover, CBM extends beyond the joint modelling of choices and response times. Its flexibility allows for the integration of diverse behavioral (e.g., confidence ratings) and biological measures (e.g., physiological responses, neural activity). As CBM captures dependencies among multiple data types, it can be applied to a wide range of cognitive tasks, broadening its utility and offering a more comprehensive representation of underlying cognitive processes.

Despite these advantages, CBM is computationally demanding, with substantially longer fitting times compared to DDM. This limitation is particularly relevant for large-scale studies or real-time applications. Additionally, while the copula framework offers flexibility, its performance is contingent on appropriate selection of marginal distributions and dependency structures. Further research should investigate best practices for parameterizing these elements across different cognitive tasks.

Limitations

Four potential limitations should be acknowledged. First, due to computational constraints, we simulated only 10 subjects completing 60 trials per paradigm. While this dataset size was sufficient to distinguish CBM from DDM, the comparison of binary choice models with and without response times revealed trends favoring response time inclusion, though statistical significance was not always achieved. Future studies should investigate whether larger datasets improve model discriminability.

Second, our CBM-derived models did not include a group-level parameter on the copula correlation, preventing pooling toward the group mean for these estimates. This decision was made due to the structure of the Lewandowski-Kurowicka-Joe distribution, which governs the copula correlation. Since this distribution only contains a single shape parameter that affects the concentration around zero, hierarchical modeling would not enable meaningful shrinkage toward the group mean. Future research could explore alternative parameterizations that facilitate hierarchical modeling of dependency structures.

Third, we only consider the Gaussian copula, which assumes a symmetric and elliptical dependency structure. Future investigations should explore alternative dependency structures to increase modeling flexibility.

Finally, while the choice models within our CBM framework are grounded in cognitive theory, our current implementation of the RT component is more simplistic and may not explicitly reflect detailed cognitive processes. This simplicity is due to our specific modeling choices rather than an inherent limitation of the CBM itself. The framework is flexible enough to incorporate more detailed cognitive interpretations depending on how it is implemented, which is an important direction for future work. Additionally, our comparisons primarily focus on the DDM; broader benchmarking against other multivariate approaches remains necessary. Although our CBM implementation outperforms the DDM in predictive accuracy across two experiments, further validation across diverse tasks is required to fully assess its generalizability.

Conclusion

In summary, CBM represents a significant methodological advancement in computational cognitive modeling. By allowing flexible integration of diverse data sources and capturing dependencies between measures. The empirical validation presented here establishes CBM as a viable and generalizable alternative to existing models, with potential applications spanning fundamental research and applied settings.

References

Bang, J. W., Shekhar, M., & Rahnev, D. (2019). Sensory noise increases metacognitive efficiency. *Journal of Experimental Psychology: General*, *148*(3), 437–452. https://doi.org/10.1037/xge0000511

Bhattacharya, A., Linero, A., & Oates, C. J. (2024). *Grand Challenges in Bayesian Computation* (arXiv:2410.00496). arXiv. https://doi.org/10.48550/arXiv.2410.00496

Carpenter, B., Gelman, A., Hoffman, M. D., Lee, D., Goodrich, B., Betancourt, M., Brubaker, M., Guo, J., Li, P., & Riddell, A. (2017). Stan: A Probabilistic Programming Language. *Journal of Statistical Software*, *76*, 1–32. https://doi.org/10.18637/jss.v076.i01

Durante, F., Fernández-Sánchez, J., & Sempi, C. (2013). A topological proof of Sklar's theorem. *Applied Mathematics Letters*, *26*(9), 945–948. https://doi.org/10.1016/j.aml.2013.04.005

Hellmann, S., Zehetleitner, M., & Rausch, M. (2023). Simultaneous modeling of choice, confidence, and response time in visual perception. *Psychological Review*, *130*(6), 1521–1543. https://doi.org/10.1037/rev0000411

Hess, A. J., Iglesias, S., Köchli, L., Marino, S., Müller-Schrader, M., Rigoux, L., Mathys, C., Harrison, O. K., Heinzle, J., Frässle, S., & Stephan, K. E. (2024). *Bayesian Workflow for Generative Modeling in Computational Psychiatry* (p. 2024.02.19.581001). bioRxiv. https://doi.org/10.1101/2024.02.19.581001

Hick, W. E. (1952). On the Rate of Gain of Information. *Quarterly Journal of Experimental Psychology*, *4*(1), 11–26. https://doi.org/10.1080/17470215208416600

Hyman, R. (1953). Stimulus information as a determinant of reaction time. *Journal of Experimental Psychology*, *45*(3), 188–196. https://doi.org/10.1037/h0056940

Klein, S. A. (2001). Measuring, estimating, and understanding the psychometric function: A commentary. *Perception & Psychophysics*, *63*(8), 1421–1455. https://doi.org/10.3758/BF03194552

Kolev, N., Anjos, U. dos, & Mendes, B. V. de M. (2006). Copulas: A Review and Recent Developments. *Stochastic Models*, *22*(4), 617–660. https://doi.org/10.1080/15326340600878206

Lewandowski, D., Kurowicka, D., & Joe, H. (2009). Generating random correlation matrices based on vines and extended onion method. *Journal of Multivariate Analysis*, *100*(9), 1989–2001. https://doi.org/10.1016/j.jmva.2009.04.008

Modrák, M., Moon, A. H., Kim, S., Bürkner, P., Huurre, N., Faltejsková, K., Gelman, A., & Vehtari, A. (2023). Simulation-Based Calibration Checking for Bayesian Computation: The Choice of Test Quantities Shapes Sensitivity. *Bayesian Analysis*, *1*(1). https://doi.org/10.1214/23-BA1404

Palmer, J., Huk, A. C., & Shadlen, M. N. (2005). The effect of stimulus strength on the speed and accuracy of a perceptual decision. *Journal of Vision*, *5*(5), 1. https://doi.org/10.1167/5.5.1

Pedersen, M. L., Frank, M. J., & Biele, G. (2017). The drift diffusion model as the choice rule in reinforcement learning. *Psychonomic Bulletin & Review*, *24*(4), 1234–1251. https://doi.org/10.3758/s13423-016-1199-y

Rahnev, D., Desender, K., Lee, A. L. F., Adler, W. T., Aguilar-Lleyda, D., Akdoğan, B., Arbuzova, P., Atlas, L. Y., Balcı, F., Bang, J. W., Bègue, I., Birney, D. P., Brady, T. F., Calder-Travis, J., Chetverikov, A., Clark, T. K., Davranche, K., Denison, R. N., Dildine, T. C., … Zylberberg, A. (2020). The Confidence Database. *Nature Human Behaviour*, *4*(3), 317–325. https://doi.org/10.1038/s41562-019-0813-1

Ratcliff, R. (1978). A theory of memory retrieval. *Psychological Review*, *85*(2), 59–108. https://doi.org/10.1037/0033-295X.85.2.59

Ratcliff, R., & Rouder, J. N. (1998). Modeling Response Times for Two-Choice Decisions. *Psychological Science*, *9*(5), 347–356. https://doi.org/10.1111/1467-9280.00067

Rescorla, R., & Wagner, A. (1972). A theory of Pavlovian conditioning: Variations in the effectiveness of reinforcement and nonreinforcement. In *Classical Conditioning II: Current Research and Theory: Vol. Vol. 2*.

Talts, S., Betancourt, M., Simpson, D., Vehtari, A., & Gelman, A. (2020). *Validating Bayesian Inference Algorithms with Simulation-Based Calibration* (arXiv:1804.06788). arXiv. https://doi.org/10.48550/arXiv.1804.06788

Vehtari, A., Gelman, A., & Gabry, J. (2017). Practical Bayesian model evaluation using leave-one-out cross-validation and WAIC. *Statistics and Computing*, *27*(5), 1413–1432. https://doi.org/10.1007/s11222-016-9696-4

Wilson, R. C., & Collins, A. G. (2019). Ten simple rules for the computational modeling of behavioral data. *eLife*, *8*, e49547. https://doi.org/10.7554/eLife.49547

Yau, Y., Hinault, T., Taylor, M., Cisek, P., Fellows, L. K., & Dagher, A. (2021). Evidence and Urgency Related EEG Signals during Dynamic Decision-Making in Humans. *Journal of Neuroscience*, *41*(26), 5711–5722. https://doi.org/10.1523/JNEUROSCI.2551-20.2021

Zhang, L., Carpenter, B., Gelman, A., & Vehtari, A. (2022). *Pathfinder: Parallel quasi-Newton variational inference* (arXiv:2108.03782). arXiv. https://doi.org/10.48550/arXiv.2108.03782

Supplementary materials

Supplementary note:

All code and analysis and models can be found on https://anonymous.4open.science/r/Hierarchical-Multivariate-Copula-Framework-D746.

Note: for the experimental data we slightly widened the standard deviations of our priors presented below and narrowed the non-decision time mean. Specifically, all group means and between subject variances' standard deviation was widened to 1 and the mean non-decision time was set to 0.2. All these priors can also be seen in the supplementary figures that display prior posterior updates i.e. supplementary figure 1-4.

Here we represent the full mathematical descriptions and priors for the computational models fit in the manuscript. Note $\mathcal{N}$ refers to the normal distribution, $\mathcal{LN}$ to the lognormal distribution, $\mathcal{N}^+$ refers to a truncated normal distribution at 0, LKJ is the Lewandowski-Kurowicka-Joe distribution, Bern represents the Bernoulli distribution, and lastly $\mathcal{C\Phi}$ referes to the guassian copula function.

Psychophysical copula based model:

$$\begin{bmatrix} F_1(B_t) \\ F_2(RT_t) \end{bmatrix} \sim \mathcal{C\Phi}\left(\begin{bmatrix} 1 & \rho_s \\ \rho_s & 1 \end{bmatrix}\right)$$

$$B_t \sim \text{Bern}(E_t)$$

$$RT_t \sim \mathcal{LN}(\mu_t, \sigma_s) + \delta_s$$

$$\mu_t = RT_{int_s} + RT_{slope_s} \cdot H(E_t)$$

$$H(E_t) = E_t \cdot log(E_t) + (1 - E_t) \cdot log(1 - E_t)$$

$$E_t = \lambda_s + (1 - 2 \cdot \lambda_s) \cdot \frac{1}{1 + \exp(-\beta_s \cdot (X_t - \alpha_s))}$$

$$\lambda_s \sim S(\mathcal{N}(\mu_\lambda, \tau_\lambda))$$

$$\alpha_s \sim \mathcal{N}(\mu_\alpha, \tau_\alpha)$$

$$\beta_s \sim exp\left(\mathcal{N}(\mu_\beta, \tau_\beta)\right)$$

$$RT_{int_s} \sim \mathcal{N}(\mu_{RT_{int}}, \tau_{RT_{int}})$$

$$RT_{slope_s} \sim \mathcal{N}\left(\mu_{RT_{slope}}, \tau_{RT_{slope}}\right)$$

$$\sigma_s \sim exp(\mathcal{N}(\mu_\sigma, \tau_\sigma))$$

$$S(x) = \frac{1}{1 + exp(-x)}$$

$rho_s \sim LKJ(12)$ $\quad$ $\delta_s \sim \mathcal{N}^+(0.3,0.05)$ $\quad$ $\mu_\lambda \sim \mathcal{N}(-3,1)$ $\quad$ $\tau_\lambda \sim \mathcal{N}^+(0.6,0.2)$

$\mu_\alpha \sim \mathcal{N}(0,5)$ $\quad$ $\tau_\alpha \sim \mathcal{N}^+(5,2)$ $\quad$ $\mu_\beta \sim \mathcal{N}(-1.5,0.5)$ $\quad$ $\tau_\beta \sim \mathcal{N}^+(0.6,0.2)$

$\mu_\sigma \sim \mathcal{N}(-1,0.25)$ $\quad$ $\tau_\sigma \sim \mathcal{N}^+(0.5,0.1)$ $\quad$ $\mu_{RT_{slope}} \sim \mathcal{N}(1.5,0.5)$ $\quad$ $\tau_{RT_{slope}} \sim \mathcal{N}^+(0.6,0.2)$

$\mu_{RT_{int}} \sim \mathcal{N}(-1,0.25)$ $\quad$ $\tau_{RT_{int}} \sim \mathcal{N}^+(0.6,0.2)$

Psychophysical drift diffusion model:

$$RT_t \sim \begin{cases} \text{Wiener}(\kappa_s, \delta_s, \eta_s, \nu_t), & B = 1 \\ \text{Wiener}(\kappa_s, \delta_s, 1-\eta_s, -\nu_t), & B = 0 \end{cases}$$

$$\nu_t = E_t - (1 - E_t) * \nu_s$$

$$E_t = \lambda_s + (1 - 2 \cdot \lambda_s) \cdot \frac{1}{1 + \exp\left(-\beta_s \cdot (X_t - \alpha_s)\right)}$$

$$\kappa_s \sim exp\left(\mathcal{N}(\mu_\kappa, \tau_\kappa)\right)$$

$$\eta_s \sim S\left(\mathcal{N}(\mu_\eta, \tau_\eta)\right)$$

$$\nu_s \sim \mathcal{N}(\mu_\nu, \tau_\nu)$$

$$\lambda_s \sim S\left(\mathcal{N}(\mu_\lambda, \tau_\lambda)\right)$$

$$\alpha_s \sim \mathcal{N}(\mu_\alpha, \tau_\alpha)$$

$$\beta_s \sim exp\left(\mathcal{N}(\mu_\beta, \tau_\beta)\right)$$

$$S(x) = \frac{1}{1 + exp(-x)}$$

$\delta_s \sim \mathcal{N}^+(0.3,0.05)$ $\mu_\lambda \sim \mathcal{N}(-3,1)$ $\tau_\lambda \sim \mathcal{N}^+(0.6,0.2)$ $\mu_\alpha \sim \mathcal{N}(0,5)$

$\tau_\alpha \sim \mathcal{N}^+(5,2)$ $\mu_\beta \sim \mathcal{N}(-1.5,0.5)$ $\tau_\beta \sim \mathcal{N}^+(0.6,0.2)$ $\mu_\kappa \sim \mathcal{N}(0.5,0.25)$

$\tau_\kappa \sim \mathcal{N}^+(0.4,0.1)$ $\mu_\nu \sim \mathcal{N}(5,0.25)$ $\tau_\nu \sim \mathcal{N}^+(0.5,0.1)$ $\mu_\eta \sim \mathcal{N}(0,0.1)$

$\tau_\eta \sim \mathcal{N}^+(0.4,0.1)$

Learning copula based model

$$\begin{bmatrix} F_1(B_t) \\ F_2(RT_t) \end{bmatrix} \sim \mathcal{C}\Phi\left(\begin{bmatrix} 1 & \rho \\ \rho & 1 \end{bmatrix}\right)$$

$$B_t \sim \text{Bern}(E_t)$$

$$RT_t \sim \mathcal{LN}(\mu_t, \sigma_s) + \delta_s$$

$$\mu_t = RT_{int_s} + RT_{slope_s} \cdot H(E_t)$$

$$H(E_t) = E_t \cdot log(E_t) + (1 - E_t) \cdot log(1 - E_t)$$

$$E_{t+1} = E_t + \alpha_s * (X_t - E_t)$$

$$\alpha_s \sim S\big(\mathcal{N}(\mu_\alpha, \tau_\alpha)\big)$$

$$E_{0_s} \sim S\left(\mathcal{N}\big(\mu_{E_0}, \tau_{E_0}\big)\right)$$

$$RT_{int_s} \sim \mathcal{N}\big(\mu_{RT_{int}}, \tau_{RT_{int}}\big)$$

$$RT_{slope_s} \sim \mathcal{N}\left(\mu_{RT_{slope}}, \tau_{RT_{slope}}\right)$$

$$\sigma_s \sim exp\big(\mathcal{N}(\mu_\sigma, \tau_\sigma)\big)$$

$$S(x) = \frac{1}{1 + exp(-x)}$$

$rho_s \sim LKJ(12)$	$\delta_s \sim \mathcal{N}^+(0.3,0.05)$	$\mu_\alpha \sim \mathcal{N}(-1,1)$	$\tau_\alpha \sim \mathcal{N}^+(0.5,0.1)$
$\mu_{E_0} \sim \mathcal{N}(0,0.2)$	$\tau_{E_0} \sim \mathcal{N}^+(0.5,0.1)$	$\mu_{RT_{slope}} \sim \mathcal{N}(1.5,0.5)$	$\tau_{RT_{slope}} \sim \mathcal{N}^+(0.6,0.2)$
$\mu_{RT_{int}} \sim \mathcal{N}(-1,0.25)$	$\tau_{RT_{int}} \sim \mathcal{N}^+(0.6,0.2)$	$\mu_\sigma \sim \mathcal{N}(-1,0.25)$	$\tau_\sigma \sim \mathcal{N}^+(0.5,0.1)$

Learning drift diffusion model

$$RT_t \sim \begin{cases} \text{Wiener}(\kappa_s, \delta_s, \eta_s, \nu_t), & B = 1 \\ \text{Wiener}(\kappa_s, \delta_s, 1-\eta_s, -\nu_t), & B = 0 \end{cases}$$

$$\nu_t = E_t - (1 - E_t) * \nu_s$$

$$E_{t+1} = E_t + \alpha_s * (X_t - E_t)$$

$$\kappa_s \sim exp\big(\mathcal{N}(\mu_\kappa, \tau_\kappa)\big)$$

$$\eta_s \sim S\left(\mathcal{N}\big(\mu_\eta, \tau_\eta\big)\right)$$

$$\nu_s \sim \mathcal{N}(\mu_\nu, \tau_\nu)$$

$$\alpha_s \sim \mathcal{N}(\mu_\alpha, \tau_\alpha)$$

$$E_{0_s} \sim S\left(\mathcal{N}\big(\mu_{E_0}, \tau_{E_0}\big)\right)$$

$$S(x) = \frac{1}{1 + exp(-x)}$$

$\delta_s \sim \mathcal{N}^+(0.3,0.05)$ $\mu_\alpha \sim \mathcal{N}(-1,1)$ $\tau_\alpha \sim \mathcal{N}^+(0.5,0.1)$ $\mu_{E_0} \sim \mathcal{N}(0,0.2)$

$\tau_{E_0} \sim \mathcal{N}^+(0.5,0.1)$ $\mu_\kappa \sim \mathcal{N}(0.5,0.25)$ $\tau_\kappa \sim \mathcal{N}^+(0.4,0.1)$ $\mu_\nu \sim \mathcal{N}(2,0.25)$

$\tau_\nu \sim \mathcal{N}^+(0.5,0.1)$ $\mu_\eta \sim \mathcal{N}(0.75,0.25)$ $\tau_\eta \sim \mathcal{N}^+(0.4,0.1)$

Supplementary Tables.

Paradigm	Model	ELPD difference	ELPD standard error	Pareto k>0.7	Pareto k>1
Psychophysics (full LL)	CBM	0	NA	2 (0.1%)	0 (0%)
Psychophysics (full LL)	DDM	-153.4	16.8	5 (0.3%)	0 (0%)
Learning (full LL)	CBM	0	NA	4 (0.04%)	1 (0.01%)
Learning (full LL)	DDM	-533.6	47.8	12 (0.13%)	8 (0.09%)
Psychophysics (Binary LL)	CBM	0	NA	0 (0%)	0 (0%)
Psychophysics (Binary LL)	Pure choice	-1.6	1.6	0 (0%)	0 (0%)
learning (Binary LL)	Pure choice	0	NA	31 (0.3%)	60 (0.6%)
learning (Binary LL)	CBM	-11.3	6.0	17 (0.2%)	71 (0.8%)

Supplementary table 1. displays the model comparison on the two experiments investigated. Expected log pointwise predictive difference (ELPD difference) of 0 indicates the winning model. The magnitude of difference in model fit is found in the losing models' ELPD difference and its associated standard error. As we used the LOO-package to compute the ELPD difference, which uses pareto smoothed importance sampling (PSIS), we obtain pareto shape parameters (k values) for each observation. These pareto k values help understand the reliability and approximate convergence rate of the PSIS-based leave one out cross validation for each observation and thus highlight highly influential observations. In general, values above 1 are viewed as very bad whereas values between 0.7 and 1 are viewed as bad. Our table shows that for our comparison between the copula-based model (CBM) and the drift diffusion model (DDM) had few if any bad diagnostics. The same was seen for the comparison on only the binary loglikelihoods (LL) for the psychophysical paradigm. Conversely, on the binary LL for the learning paradigm we had quite a few diagnostics above 1, which warrants caution for interpretation.

Supplementary Figures.

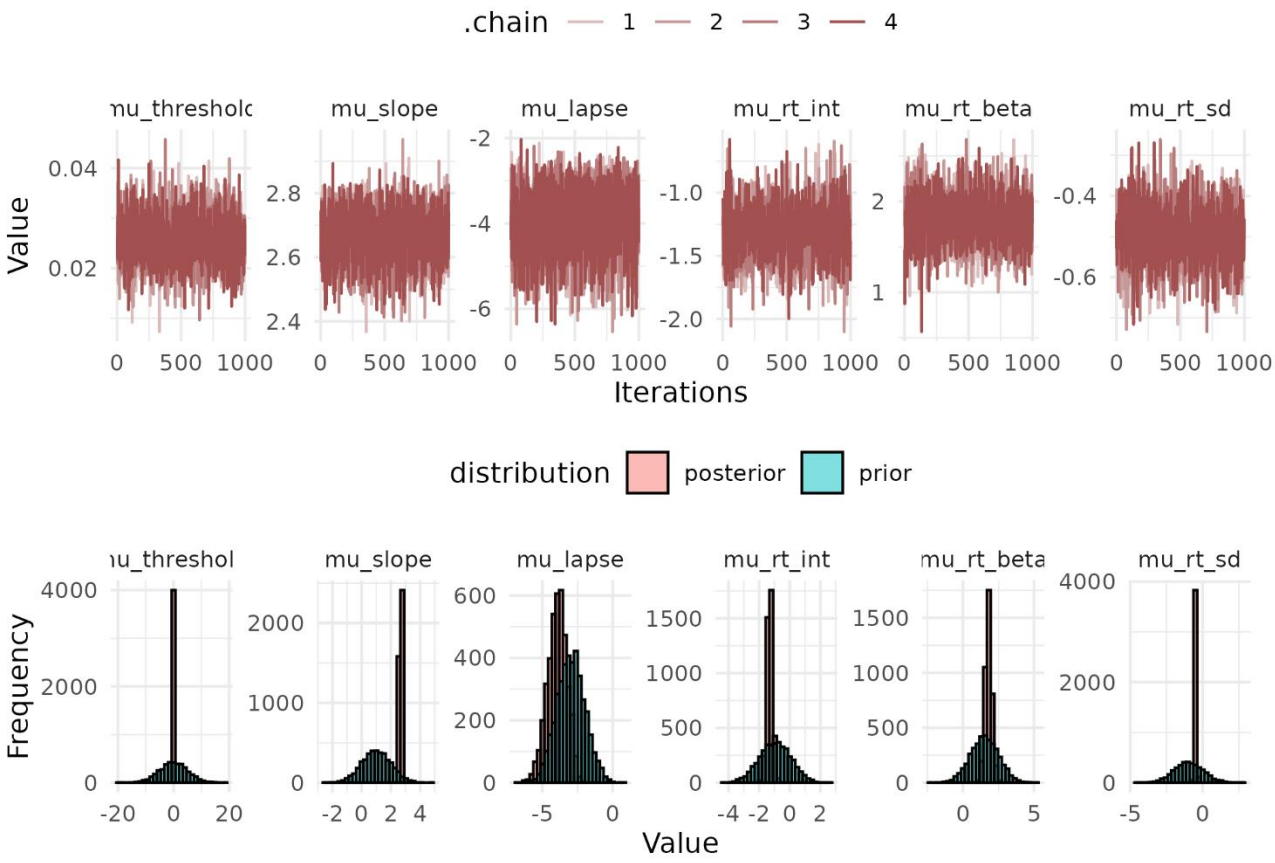

Supplementary figure 1. *Displays traceplots (upper) and prior posterior updates (lower) for each group mean parameter for our derived multivariate hierarchical copula based model for the experimental data from the psychophysical paradigm.*

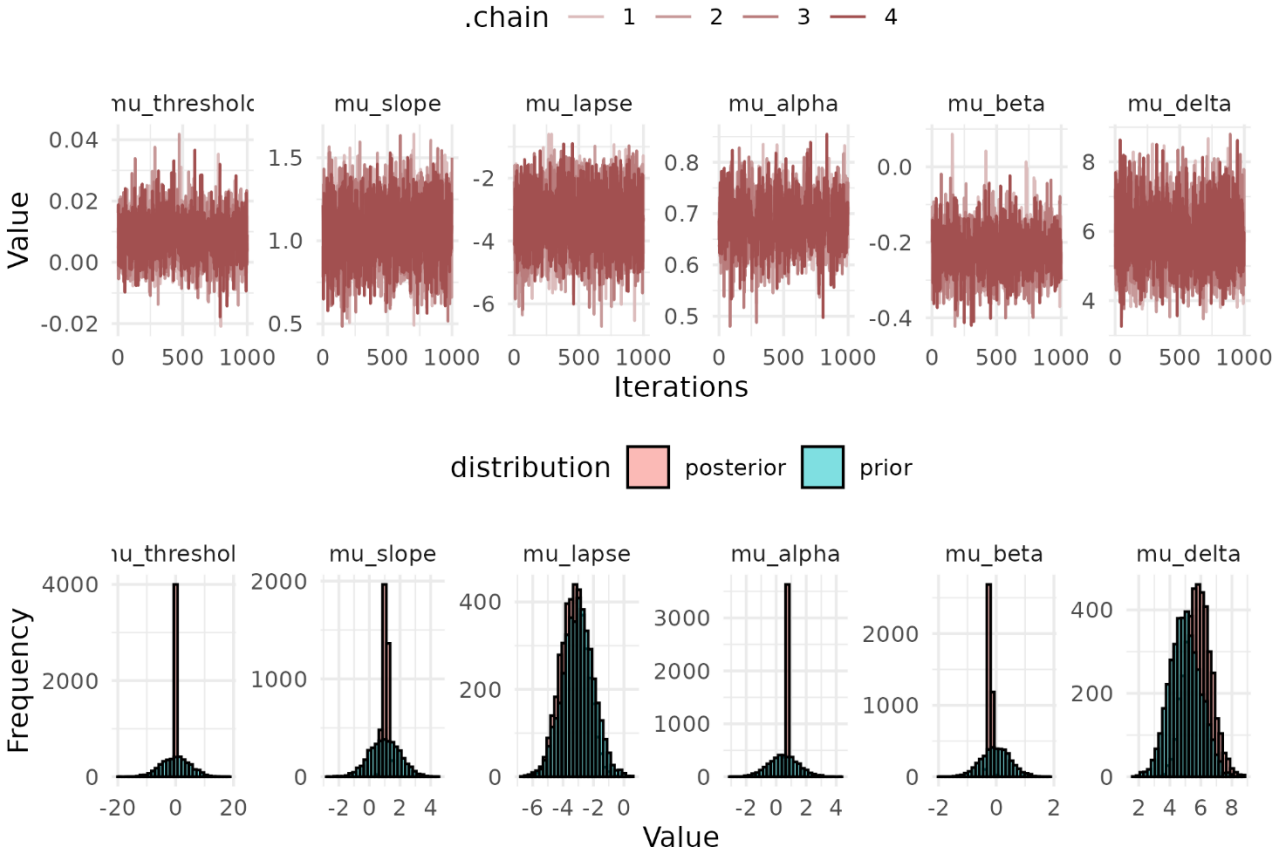

Supplementary figure 2; Displays traceplots (upper) and prior posterior updates (lower) for each group mean parameter for the drift diffusion model for the experimental data from the psychophysical paradigm.

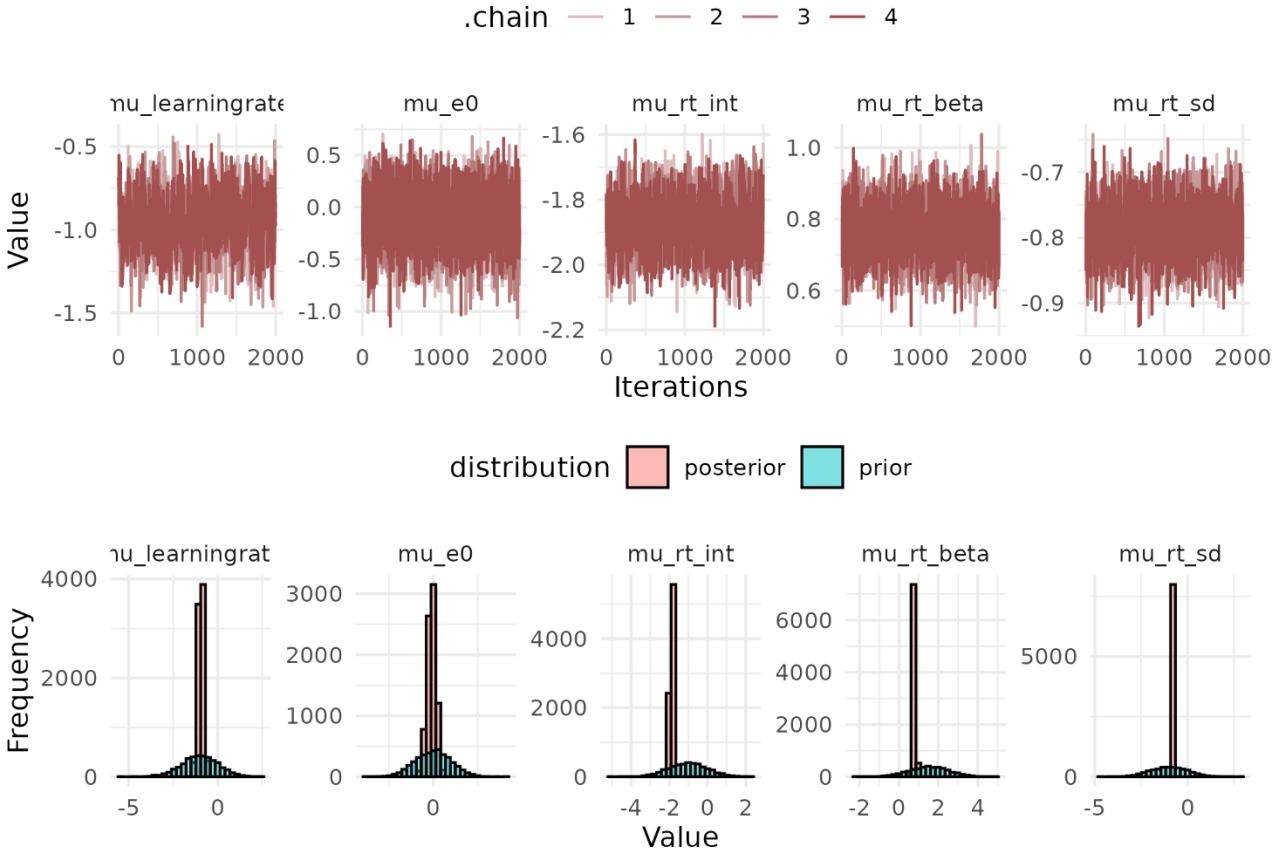

Supplementary figure 3. *Displays traceplots (upper) and prior posterior updates (lower) for each group mean parameter for our multivariate hierarchical copula based model for the experimental data from the probabilistic learning paradigm.*

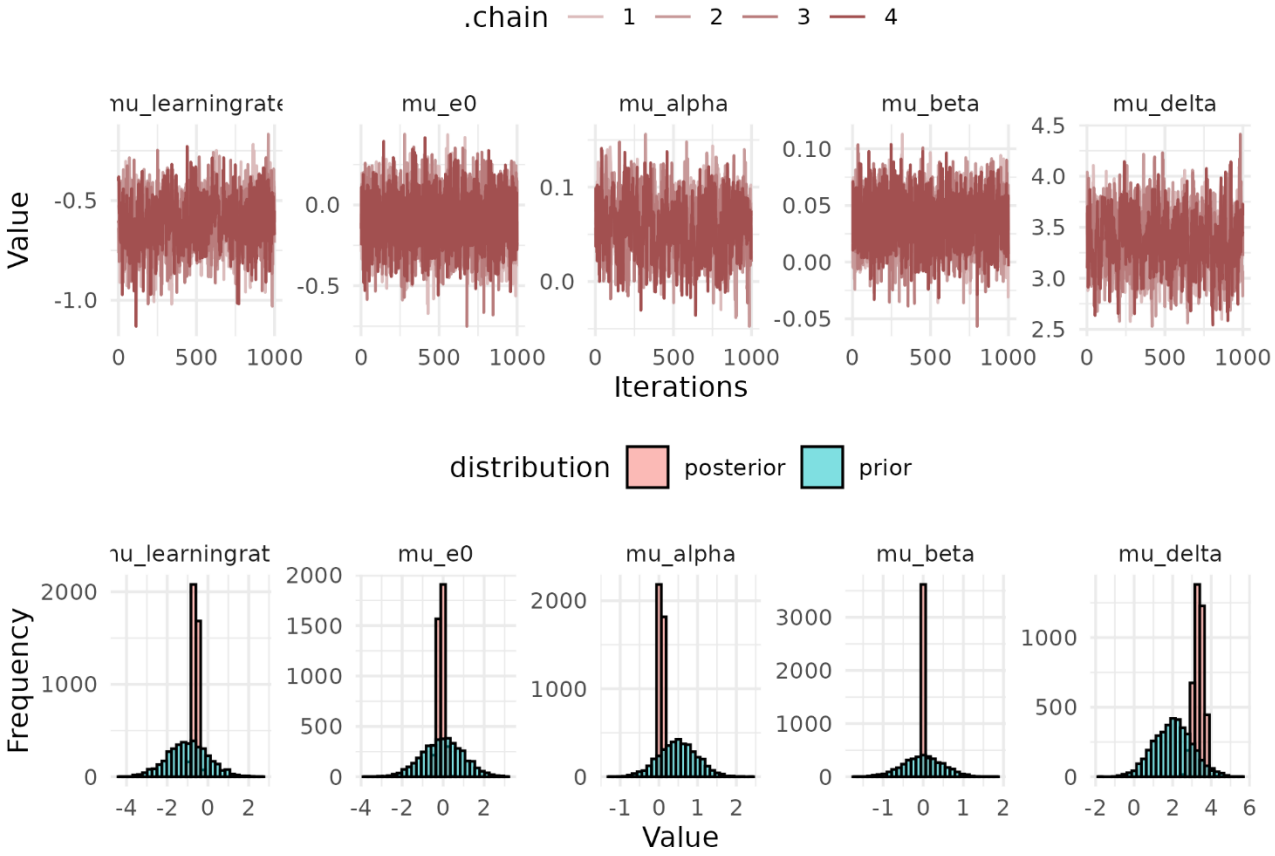

Supplementary figure 4. *Displays traceplots (upper) and prior posterior updates (lower) for each group mean parameter for the drift diffusion model for the experimental data from the probabilistic learning paradigm.*

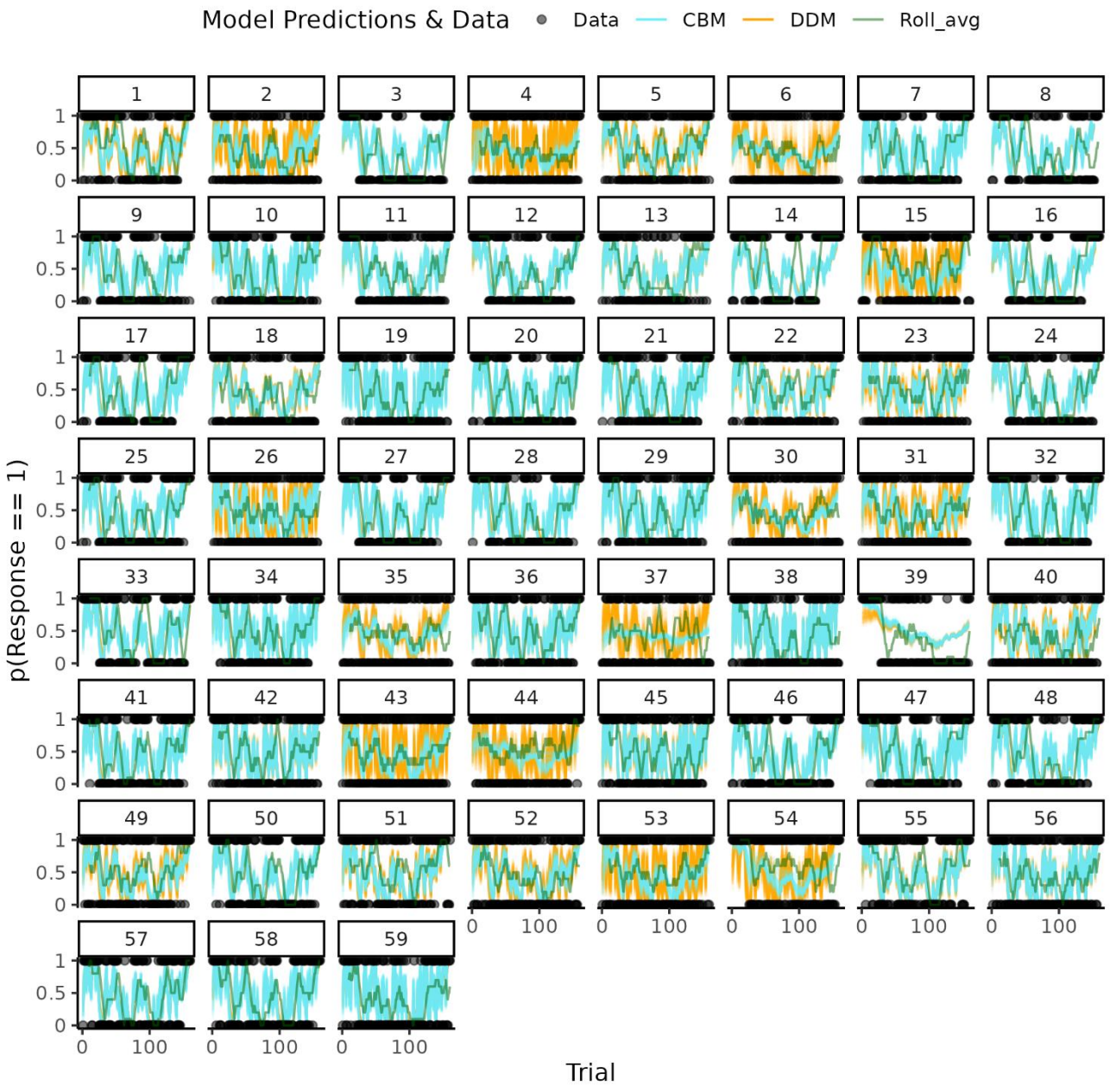

Supplementary figure 5. *Displays subject level posterior predictive distributions for the CBM and DDM framework to the probabilistic learning paradigm with trial number on the x-axis and the probability of responding one, on the y-axis. Black dots represent the individual subjects' binary choices whereas the green line represents the rolling average of 10 of these binary choice. Each facet represents a subject.*

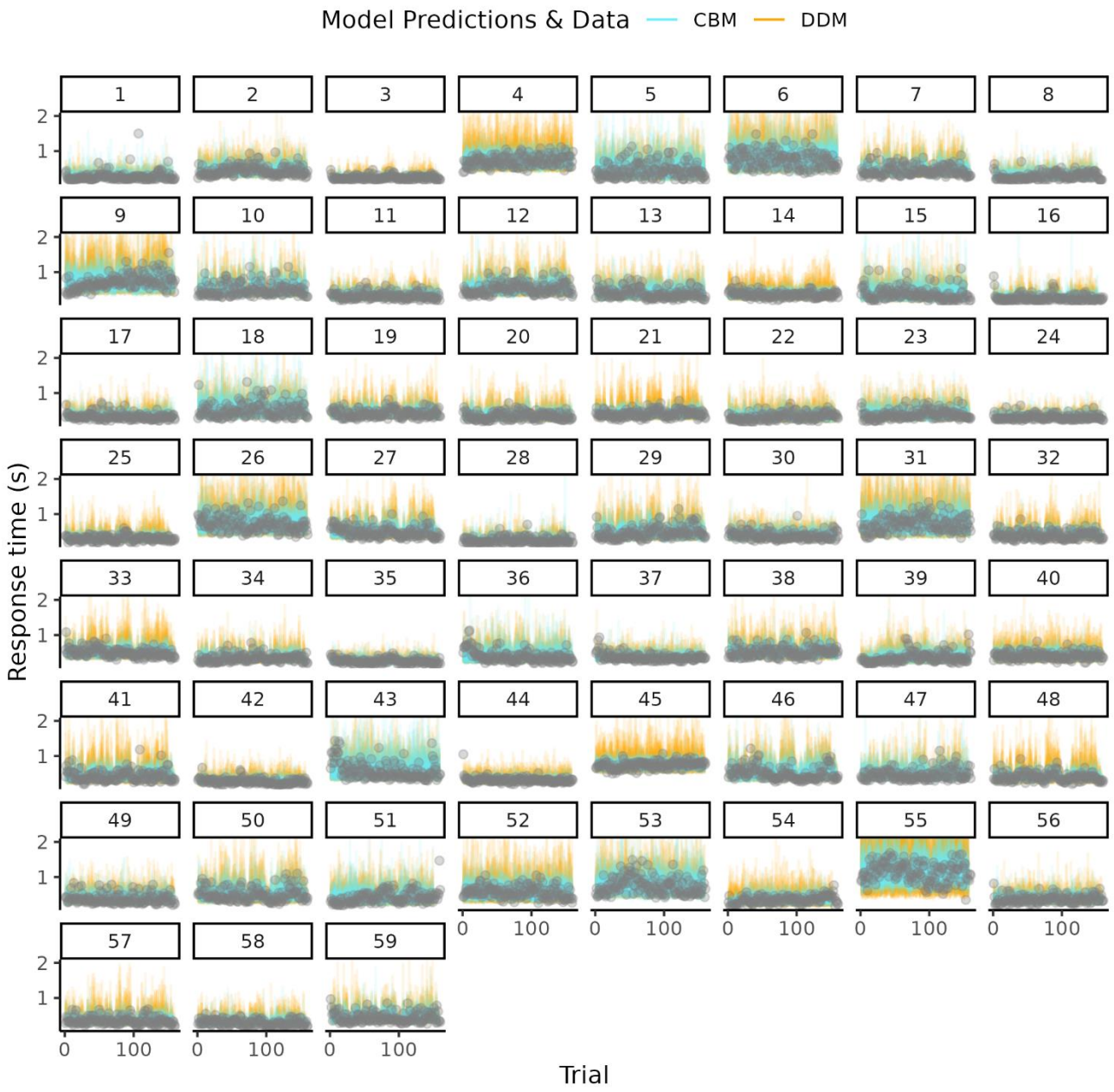

Supplementary figure 6. *Displays subject level posterior predictive distributions for the CBM and DDM framework to the probabilistic learning paradigm with trial number on the x-axis response times on the y-axis. Black dots represent the individual subjects' binary choices. Each facet represents a subject.*

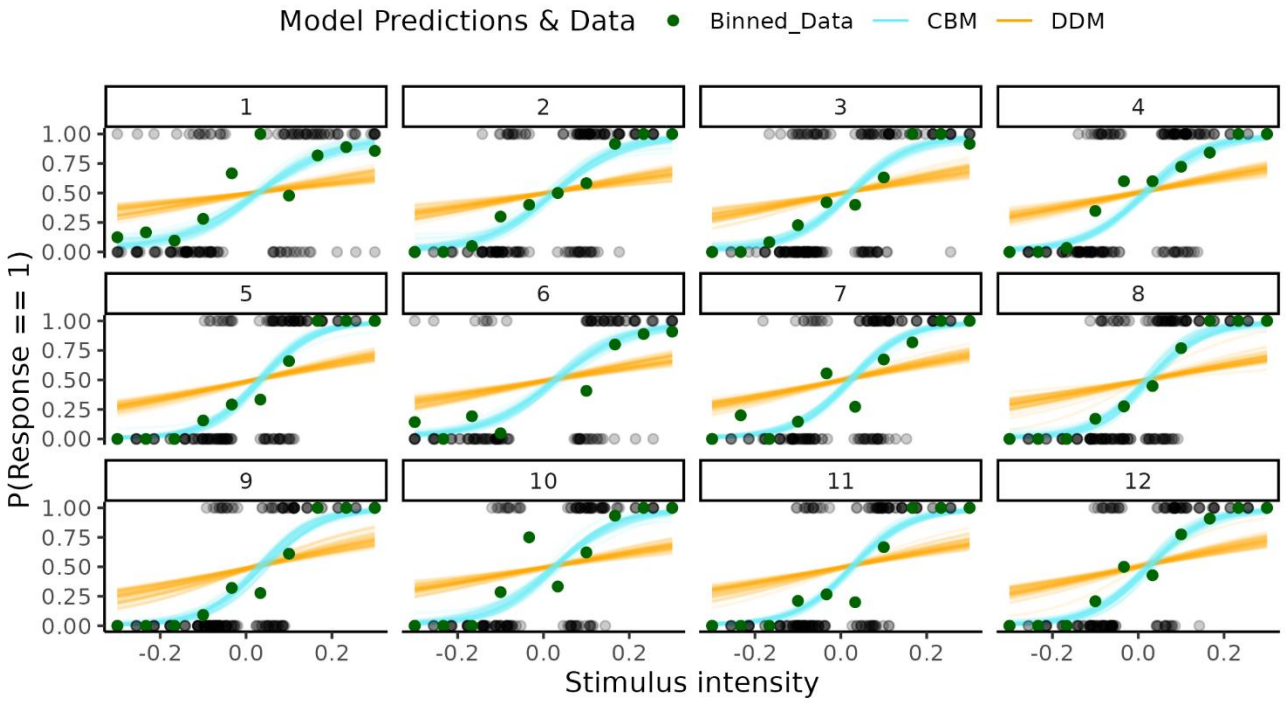

Supplementary figure 7. *Displays subject level posterior predictive distributions for the CBM and DDM framework to the psychophysical paradigm with stimulus intensity on the x-axis and the probability of responding one, on the y-axis. Black dots represent the individual subjects' binary choices whereas the green dots represent equally sized bins of the stimulus intensity of binary responses. Each facet represents a subject.*

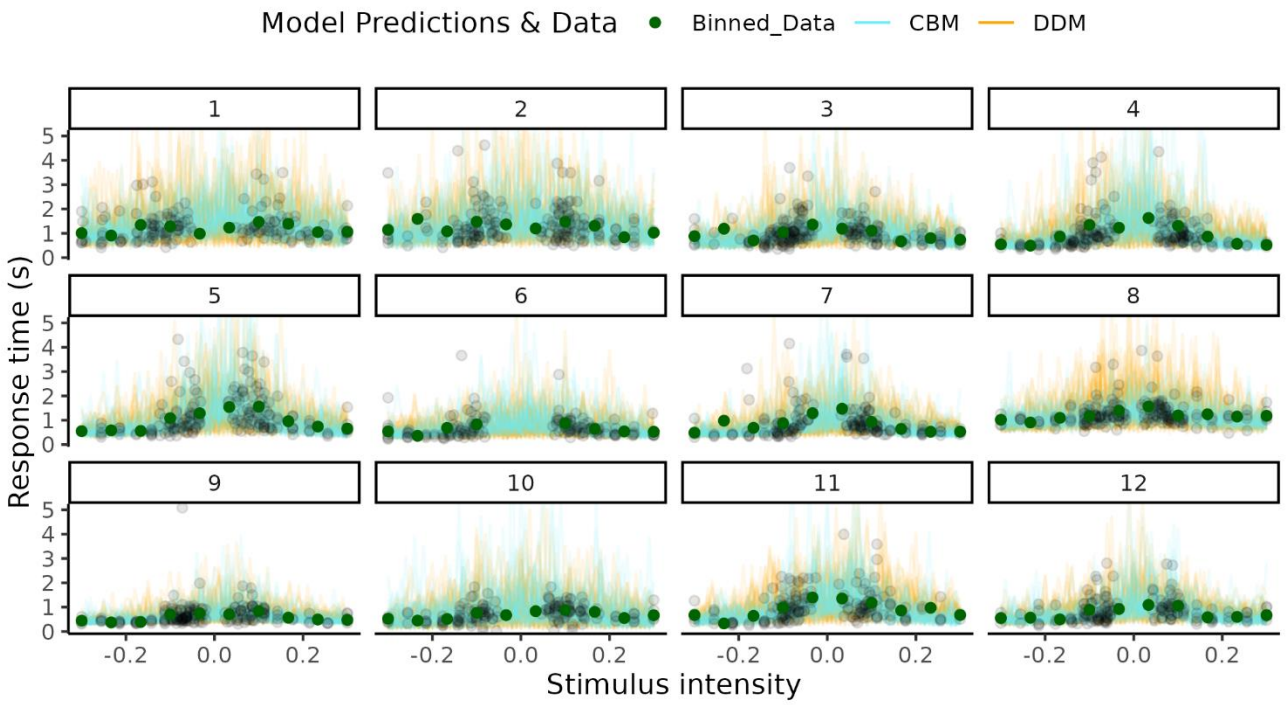

Supplementary figure 8. *Displays subject level posterior predictive distributions for the CBM and DDM framework to the psychophysical paradigm with stimulus intensity on the x-axis and response times on the y-axis. Black dots represent the individual subjects' binary choices whereas the green dots represent equally sized bins of the stimulus intensity of response times. Each facet represents a subject.*

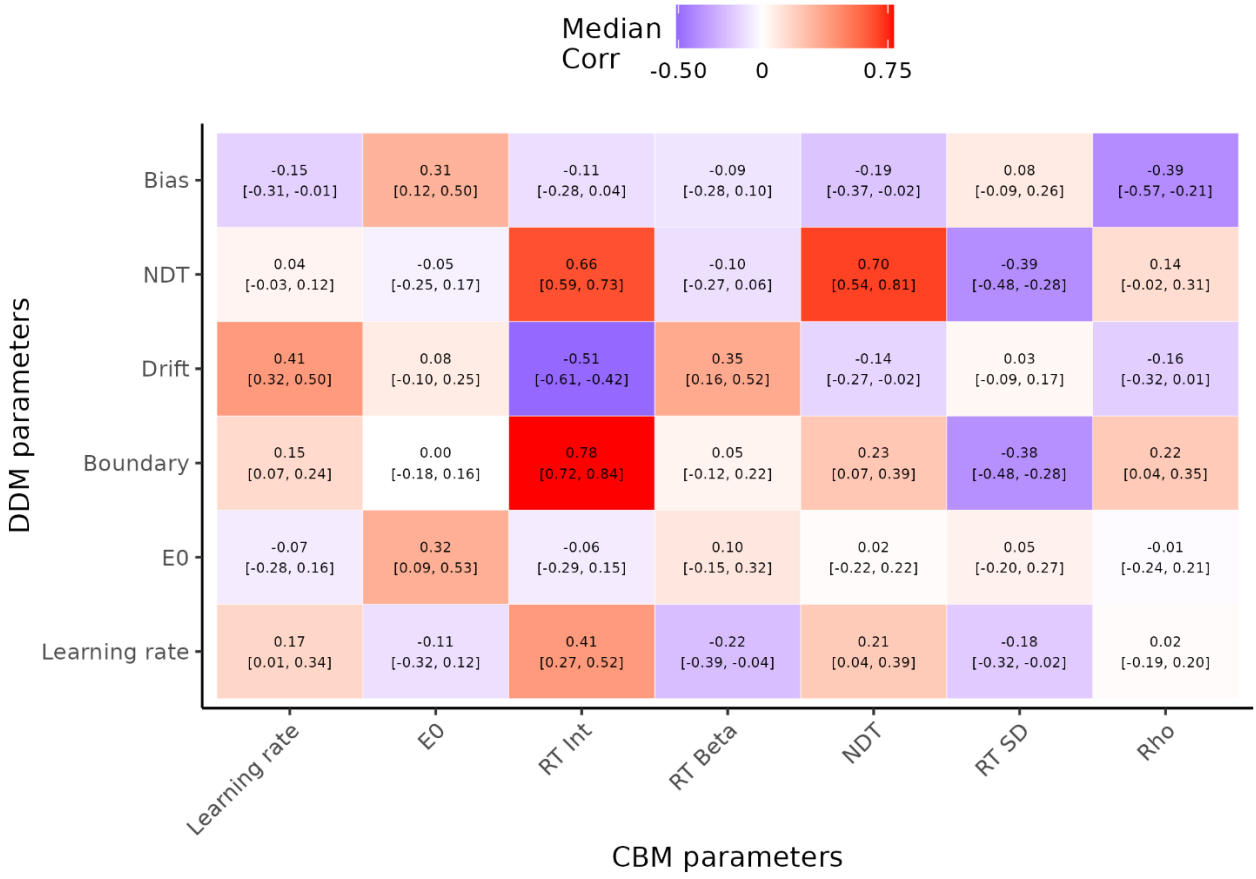

Supplementary figure 9. *Displays subject level correlation of the parameters of the DDM and CBM model fits to the probabilistic learning paradigm. Numbers in each cell represent the median correlation with its 95% highest density interval in the square brackets.*

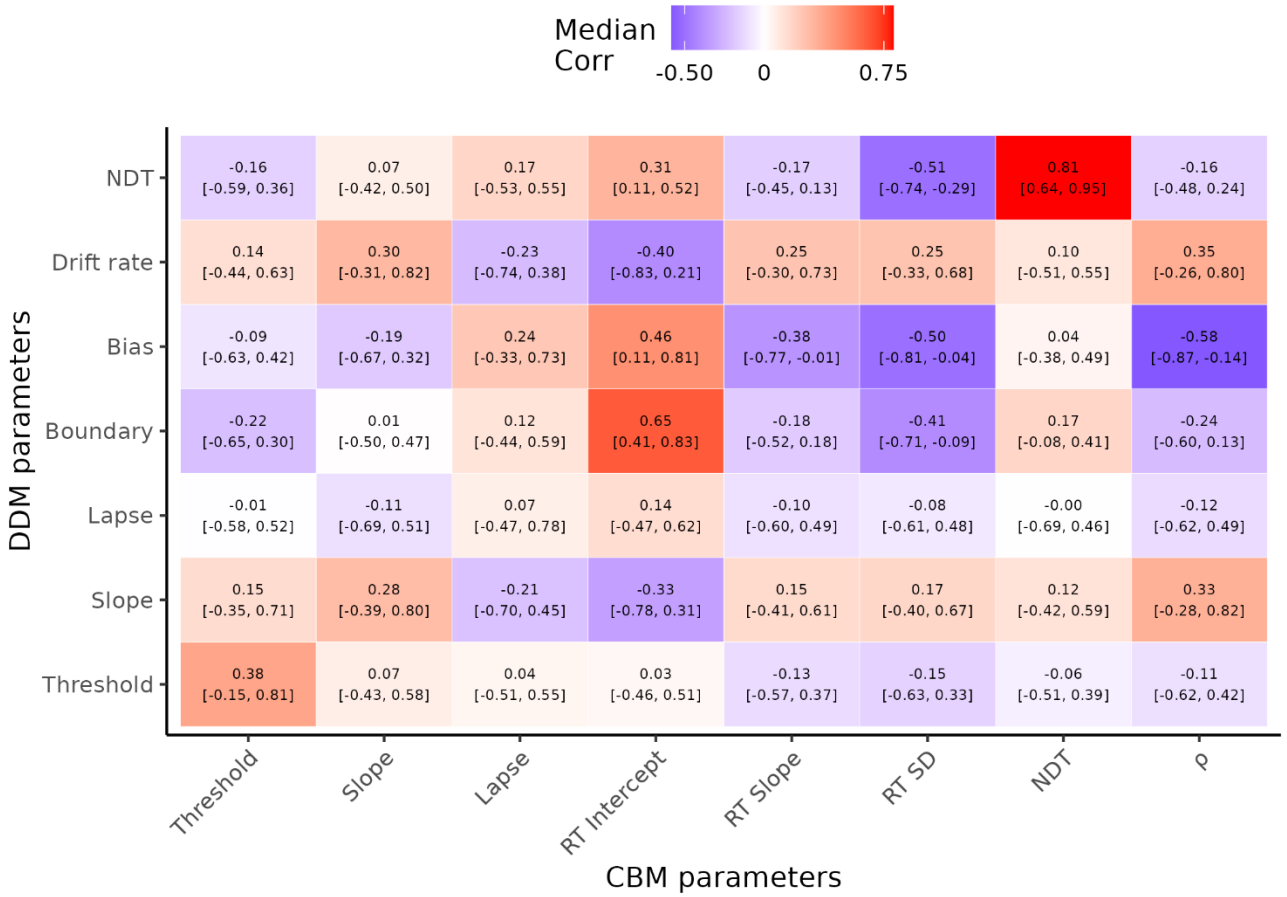

Supplementary figure 10. *Displays subject level correlation of the parameters of the DDM and CBM model fits to the psychophysical paradigm. Numbers in each cell represent the median correlation with its 95% highest density interval in the square brackets.*